Mineralium Deposita (1997) 32: 607–616

ARTICLE

W.H. MacLean · F.F. Bonavia · G. Sanna

Argillite debris converted to bauxite during karst weathering: evidence from immobile element geochemistry at the Olmedo Deposit, Sardinia

Received: 10 June 1996 / Accepted: 15 April 1997

Abstract The Olmedo bauxite deposit occurs in the Nurra district of northwest Sardinia. It forms a stratiform horizon in Cretaceous limestone and marl. Uplift in mid-Cretaceous had exposed recently deposited limestone to karst weathering, and a layer of argillaceous debris accumulated on its surface and was partly converted to bauxite. Intermediate products were desiccated marl, bauxitic argillite and argillaceous bauxite. Subsidence followed, and the bauxite was preserved by the deposition of late Cretaceous limestone and other sediments. Uplift in Oligocene-Miocene time, with ensuing erosion, exposed the bauxite horizon to its present configuration. Concentrations of normative minerals illustrate chemical processes and the build-up of Al in the bauxite horizon. Plots of chemical data and correlation coefficients show that Al, Ti, Zr, Nb, Th, Cr and V were immobile during the bauxitization process. Mass changes point to large net removal of Si, Mg and K from the system, although some of this material and slightly mobile Al were reprecipitated in the underlying argillite and altered marl. Immobile element ratios trace the source of the bauxite to the underlying argillaceous limestone. Al in the bauxite was accumulated from the degradation of 25 to 50 m of the argillaceous limestone.

Introduction

The source of the Al in some bauxite deposits has long been a subject of debate (Gow and Lozej 1993). Many bauxites can be directly related through textures and chemistry to underlying bedrock, but for those above sedimentary limestone sequences there is a wider selection, from argillite components of underlying limestone, to fluvially transported basement rock debris (e.g., Bardossy 1982, 1984), and deposits of volcanic ash (Bardossy 1984, Lyew-Ayee, 1986). In all these models Al is concentrated in situ as inert (immobile) lateritization residue. In other deposits Pye (1988) and Brimhall et al. (1988) have proposed windborne transport as the re-concentration process that forms local high-grade bauxites.

Bauxite deposits in the Nurra district, northwest Sardinia (Fig. 1), are in sequences of limestones and marls that have a complex history of deposition, uplift, subaerial erosion and karst weathering (Cocco and Pecorini 1959; Oggiano et al. 1987). Following Bardossy (1982, 1984), these deposits are classified as "Mediterranean type" or possibly "Ariege type" with a "karst type" developed only at the margin.

In the residual accumulation of bauxite ores, Al has historically been recognized as an immobile element (e.g., Sastri and Sastry 1982; Valeton et al. 1987; Gow and Lozej 1993). With this element alone, however, it is not possible to trace the source of the Al to a particular rock type or unit, or to make precise mass balance calculations for the bauxitization process (MacLean 1990). It is now known that elements like Ti, Zr, Nb, Th and Cr are immobile in some forms of hydrothermal alteration around metallic ore deposits (MacLean and Kranidiotis 1987; MacLean and Barrett 1993), and their distribution can be used to identify precursor rocks. Immobile element geochemistry techniques may therefore help to choose the deposit "type" and identify the source rocks which are important factors in bauxite formation.

In this study Ti, Zr, Nb, Th and Cr are shown to have been immobile in the formation of the Olmedo deposit. They are used to investigate the nature of the bauxite precursor, follow the various stages of the bauxitization process, and quantify the losses and gains of mass during each stage of bauxite formation.

Editorial handling: D.J. Morgan

W.H. MacLean (✉)
Department of Earth and Planetary Sciences,
McGill University, Montreal, Canada H3A 2A7

F.F. Bonavia
Departement de Géotectonique (URA 1759),
Université Pierre-et-Marie Curie, Paris, France

G. Sanna
PROGEMISA, via Contivecchi 7, 09122 Cagliari, Italy

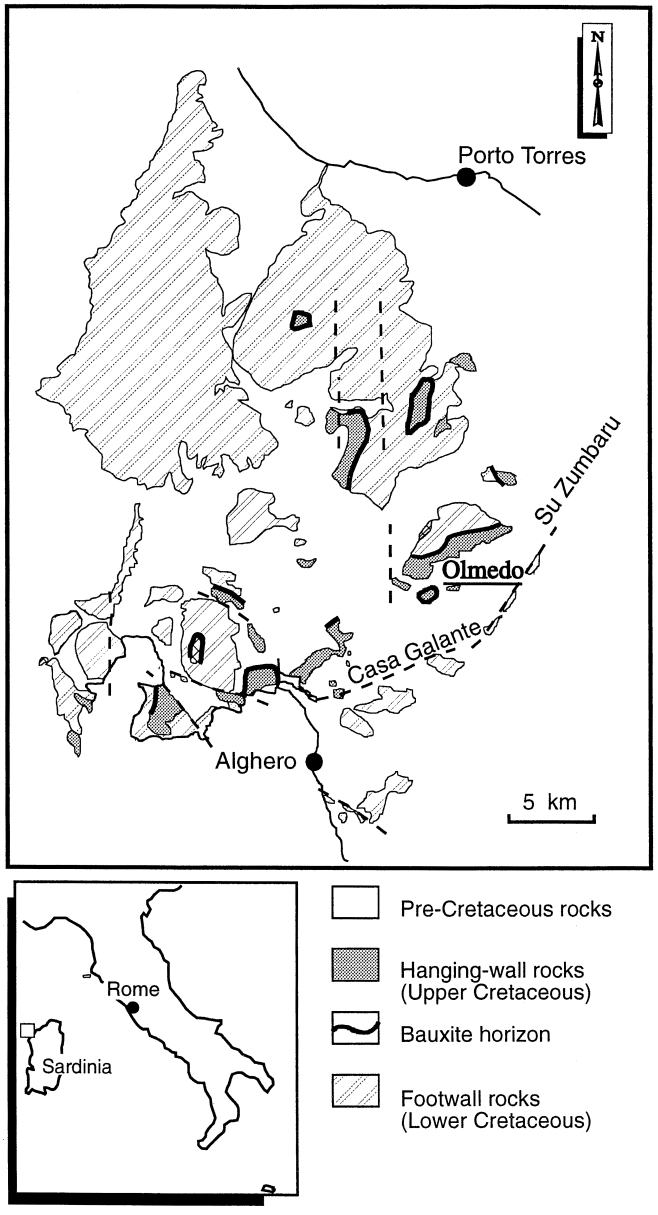

Fig. 1 Geological map of northeast Sardinia showing position of bauxite occurrences (after Sanna and Temussi, 1986)

Olmedo geology

The Olmedo bauxite forms a stratiform unit within sequences of Cretaceous marine carbonates deposited up to mid-Cretaceous (Cocco and Pecorini 1959; Sanna and Temussi 1986). Footwall rocks are predominantly lagoonal-lacustrine marls and intraclastic carbonates typical of internal marine platforms (Purbeckian facies). Also present are intrasparitic limestones with thin layers of oolites (Urgonian facies), marking the time span from Valanginian to Barremian (Fig. 2b).

In mid-Cretaceous the area was uplifted and a karst erosional surface formed under climatic conditions favorable to bauxite formation. The Case Galante-Su Zumbaru tectonic lineament was developed at this time with subsidiary renewed movement along Late Herycnian basement faults (N60E and N150E, Figs. 1, 2a). In the Late Cretaceous, the region subsided and marine limestones and marls were deposited on the bauxitic horizon. Overlying units

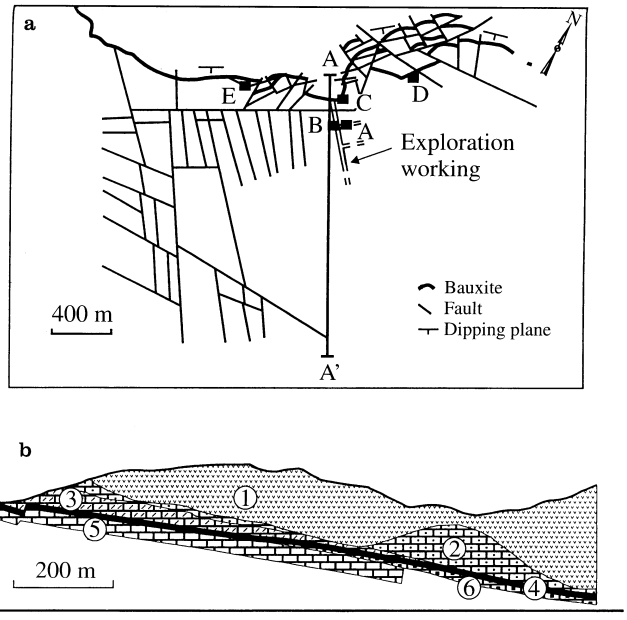

Fig. 2 a Sketch map with sampling sites (*A*, *B*, *C*, *D* and *E*); **b** geological cross section (*A*-*A*', on plan map) (after Sanna and Temussi 1986). Key: *1*, volcanic (Oligo-Miocene); *2*, calcarenite and marl (Santonian); *3*, bioclastic limestone (Upper Coniacian); *4*, bauxite horizon; *5*, limestone (Upper Valanginian); *6*, marl, calcareous marl and limestone (Lower Valanginian – Upper Berriasian)

of the stratigraphy are a thin biosparitic limestone (platform deposition) or a thick bioclastic limestone (deposited in the interior parts of the platform), a thick and widespread succession of yellow to gray-black marls and calcarenites, rare occurrences of green marl, covered by lenses of tuff, ignimbrite, ash and altered volcanic products.

Uplift in Oligocene-Miocene time and ensuing erosion exposed the bauxite horizon in its present state. The Case Galante-Su Zumbaru tectonic line marks the southern boundary of bauxite occurrences in the Nurra. The bauxite horizon crops out continuously over a strike length of about 4 km (Fig. 2a), and has a fairly uniform thickness averaging 2.6 m (max. 5 m). It trends ENE, and dips about 20° to the SSW (Fig. 2b). Estimated reserves are 30 million tonnes grading 60% Al_2O_3 (dry basis).

Methods

Fifty-two samples were collected for chemical analyses from five profiles across the bauxite horizon (A, B, C, D, E, Fig. 2a) exposed in exploration workings. Portions of the samples were analyzed for major and trace elements at the Department of Earth and Planetary Sciences, McGill University by X-ray fluorescence methods using a Philips Model 1240 spectrometer. Major elements, V, Cr and Ba were analyzed using sample powders fused with a Li-tetraborate flux, and Rb, Sr, Y, Zr, Nb and Th using pressed powder pellets. Accuracy is $\pm 0.5\%$ of the amount of each major element present, and $\pm 2\%$ of each trace element. A Rigaku D/Max 2400 (12 KW) X-ray diffraction (XRD) spectrometer was used to identify minerals in selected samples.

The bauxite has high Al, Si, Fe, Ti, Zr, Nb, Cr and a few other trace elements. Some of these (Al, Ti, Zr, Nb, Th, etc.) were immobile and their concentrations enhanced during the bauxitization process. Other elements, such as Fe and Ni, were slightly mobile, and their concentrations are erratic. K, Mg, Si and most other major and trace elements were mobile and largely depleted from the bauxite. The ratios of immobile elements such as Al/Ti and Ti/Zr

will be the same in the bauxite as in the precursor rock (see Valeton et al. 1987), and thus can be used to distinguish between different source rocks (e.g., limestone versus fluviatile sediment). These ratios produce characteristic highly correlated ($R > 0.9$) linear arrays (alteration lines) that pass through the origin of the plot. Only when these conditions are fulfilled can elements be considered immobile (MacLean 1990).

Immobile elements can be used to quantify chemical modifications and mass changes that take place during an alteration process (MacLean and Kranidiotis 1987; MacLean and Barrett 1993). The changes in the mobile element components are calculated against an immobile element, Ti in the following example. An *enrichment factor* (EF) is first calculated for each sample

$$EF = \mathrm{TiO_{2\ limestone}}/\mathrm{TiO_{2\ altered\ sample}} \quad (1)$$

and *reconstituted compositions* (RC) are computed for each rock component

$$RC = EF \times \text{wt.\% oxide in the sample.} \quad (2)$$

Parts per million or other units can be substituted for weight% when dealing with trace elements. The *mass changes* are:

$$\text{Mass change} = RC - \text{precursor.} \quad (3)$$

Mineralogy and texture

The bauxite deposit profile constitutes a basal limestone and overlying desiccated marl and argillite passing upwards through bauxitic argillite, argillaceous bauxite and compact red and white bauxite (Fig. 3). Calcite and minor dolomite constitutes up to 25% of the altered marl, and the remainder of this unit and the overlying argillite are visibly composed largely of illite, kaolinite, montmorillonite, quartz, hematite and minor goethite. The minerals identified by XRD are listed in Table 1. Although detected in the field and in hand samples, quartz or other silica minerals were not detected by XRD. However, XRD profiles of samples containing 'quartz' have anomalously high backgrounds which may indicate X-ray scattering from an amorphous silica component. Quartz is also a major normative component of the argillite units (see later).

Table 1 Minerals in units of the Almedo bauxite horizon identified by X-ray diffraction spectroscopy

Unit (sample number)	Minerals identified	
	Major	Minor
White bauxite (A1-9)	Boehmite	Kaolinite, anatase
Red bauxite (A1-7)	Boehmite	Kaolinite, hematite, goethite
Bauxitic argillite (D3)[a]	Kaolinite > boehmite	Illite, goethite, hematite
Argillite (A1-6)[a]	Kaolinite > illite	Goethite, hematite
Argillite (A1-4)[a]	Kaolinite > illite	Goethite
Marl (B1-3)[a]	Calcite, kaolinite, illite	Goethite, dolomite
Limestone (A1-1)	Calcite≫dolomite	Illite, kaolinite

[a] Anomalously high X-ray background, probably due to an amorphous silica component

The bauxitic argillite is an identifiable and mappable unit where quartz has disappeared, illite is depleted, kaolinite enhanced, and boehmite (gibbsite is rare in the deposit) makes its appearance. The argillaceous bauxite is essentially a mixture of kaolinite, boehmite with variable hematite (goethite is subordinate), and this grades into red (hematite-rich) and then to white bauxite as kaolinite and hematite decrease and boehmite becomes the dominant mineral. Oolites and pisolites of boehmite and hematite are common. Oolites are small in the white bauxite and form a micro-oolitic texture, which grades to homogeneous compact bauxite as hematite is leached and the oolitic texture is masked. Titanium is present mainly as anatase which crystallized during bauxitization, and subordinate rutile of a detrital origin. Zircon is always detrital. The white bauxite is commonly covered by a thin (< 1 m) conglomeratic bauxite with a matrix of Late Cretaceous limestone.

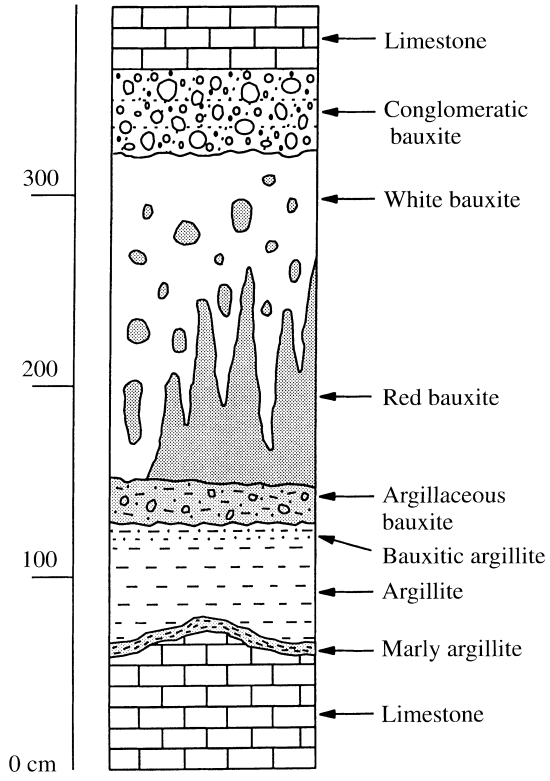

Geochemistry

Bulk chemistry

Average chemical analyses for units of the five sampled bauxite profiles are listed in Table 2a. The basal limestone contains a small "argillite" component (Si, Al, Fe, Mg, K), whereas the marl averages about 10% carbonate and 90% argillite. The argillite and bauxitic argillite have remarkably similar compositions, but K and Mg are lower in the latter, and this, as shown later, has a

◀

Fig. 3 A general geological sampling profile through the bauxite horizon. The characteristic features are listed along with averages and ranges in thickness of the sampled units. From top to bottom: *hanging wall limestone* (Late Cretaceous); 40 cm (0–50) of *conglomeratic bauxite* with a matrix of late Cretaceous limestone; 170 cm (50–400) of mature, compact, oolite-pisolite textured *white and red bauxite* in a matrix of fine alluvial bauxite fragments; reddish-ochre bauxite at the base grades into overlying white bauxite; 15 cm (5–25) of *argillaceous bauxite*, containing nodules with higher iron content (red argillaceous bauxite), with gradual transition over a few cm into overlying bauxite; 60 cm (10–150) of *argillite*, predominantly kaolinite and sericite (illite) with subordinate quartz, hematite (goethite), anatase, and nodules of low-iron boehmite, grading upward to bauxitic argillite; 10 cm (5–20) of *marl* (yellow marly argillite); *limestone* (Middle Cretaceous) argillaceous, grading to decomposed marly limestone in the upper few centimeters

Table 2 Chemical compositions of units of the Olmedo bauxite stratigraphy. Major elements and LOI in wt.%, trace elements in ppm

a Average chemical composition

Rock type	Limestone	Marl	Argillite	Bauxite argillite	Argillite bauxite	Red bauxite	White bauxite	Conglomerate bauxite
SiO_2	5.47	39.78	42.14	38.79	26.99	6.81	4.91	21.69
TiO_2	0.20	1.23	1.36	1.54	2.47	3.11	4.02	2.43
Al_2O_3	3.99	26.32	28.70	32.41	46.89	59.48	71.97	49.28
Fe_2O_3	1.06	5.95	11.02	12.72	8.24	16.45	5.23	10.63
MnO	0.03	0.02	0.03	0.02	0.02	0.02	0.02	0.01
MgO	0.92	1.56	1.38	0.42	0.14	0.07	0.18	0.17
CaO	48.86	6.77	0.75	1.14	0.71	0.74	0.22	0.86
Na_2O	0.02	0.05	0.04	0.02	0.00	0.00	0.00	0.00
K_2O	0.30	3.01	3.06	1.33	0.24	0.10	0.15	0.16
P_2O_5	0.02	0.08	0.08	0.05	0.04	0.05	0.04	0.04
CO_2[a]	38.34	5.32	0.59	0.90	0.56	0.58	0.17	0.67
Sum	99.21	90.08	89.16	89.32	86.29	87.40	86.91	85.95
LOI[b]	1.13	10.47	11.60	11.58	13.42	13.44	13.25	14.61
V	41	189	210	260	397	616	456	461
Cr	41	288	248	307	623	902	984	727
Ni	23	125	167	162	101	93	64	94
Ba	110	359	300	299	134	170	123	106
Rb	26	135	137	60	12	5	10	10
Sr	143	116	123	83	60	56	67	34
Y	44	146	115	52	49	67	73	48
Zr	44	249	297	337	538	671	869	587
Nb	5	24	27	30	53	61	83	52
Th	5	24	26	30	39	59	60	48

[a] calculated from CaO as calcite
[b] LOI less calculated CO_2

b Chemical analyses of the bauxite units normalized to a carbonate and water free basis

Rock type	Limestone	Marl	Argillite	Bauxite argillite	Argillite bauxite	Red bauxite	White bauxite	Bauxite Conglomerate
SiO_2	46.58	51.02	47.97	44.44	31.75	7.91	5.68	25.69
TiO_2	1.73	1.57	1.55	1.77	2.91	3.61	4.65	2.88
Al_2O_3	33.99	33.75	32.68	37.13	55.14	69.11	83.18	58.37
Fe_2O_3	9.05	7.62	12.55	14.58	9.70	19.10	6.04	12.59
MnO	0.26	0.03	0.03	0.02	0.02	0.02	0.02	0.02
MgO	5.52	2.00	1.57	0.48	0.16	0.08	0.20	0.21
CaO	0.00	0.00	0.00	0.00	0.00	0.00	0.00	0.00
Na_2O	0.14	0.06	0.06	0.00	0.00	0.00	0.00	0.00
K_2O	2.58	3.85	3.49	1.52	0.28	0.11	0.18	0.19
P_2O_5	0.15	0.10	0.10	0.06	0.04	0.06	0.05	0.05
CO_2	0.00	0.00	0.00	0.00	0.00	0.00	0.00	0.00
V	350	242	239	298	466	716	573	546
Cr	239	252	193	241	501	717	799	598
Ni	196	161	191	186	119	108	74	112
Ba	842	413	306	306	141	177	118	113
Rb	218	173	156	69	14	6	10	12
Sr	1215	148	140	95	70	65	65	41
Y	374	187	131	60	58	78	84	57
Zr	372	319	338	386	633	779	1005	696
Nb	39	31	30	35	62	71	96	62
Th	43	30	30	34	46	69	69	56

significant effect on their mineralogy and physical appearance. The argillaceous bauxite and bauxite are essentially devoid of K and Mg, but Al and Ti are enriched, Fe is erratic, and Si is strongly depleted. Fe is concentrated in the red bauxite relative to the argillic and white bauxite. Mn, Na and P are very low and unvarying in all parts of the stratigraphy. Al, Ti and trace elements V, Cr, Zr, Nb and Th are enriched upward through all parts of the bauxite profile. Y, Sr, Rb, Ba and Ni reach maxima in the altered marl and argillite and then fall off to constant low contents in bauxite.

Carbonate-free chemistry

The changes in chemical composition from limestone and altered marl to argillite can largely be explained by decrease in the carbonate content. When the chemical

analyses are recalculated to a carbonate-free basis (minus Ca and CO_2, assuming $CaCO_3$ as the lone carbonate component), the residual components for the three units have remarkably similar values (Table 2b). The high MgO, Ba and Sr contents of the calculated argillite residue of the limestone are the greatest discrepancies, indicating that the three probably formed carbonate components. Color and textural varieties of the argillite are not all chemically distinctive. The similarity in non-carbonate bulk chemistry suggests, but does not rigorously prove, that the argillite units and the argillite component of the limestone are the same material.

Although there is close chemical identity of the argillite component among the lower units, the relationship of the argillite to the overlying bauxite is not at all clear from the bulk chemistry. The diminishment to near elimination of many major and trace elements across the argillite-bauxite boundary makes a cursory comparison impossible.

Normative mineralogy

The chemical changes in the lateritization process can also be viewed as changes in mineralogy. Visual modal estimates are difficult to make in these fine-grained rocks, and XRD estimates were hampered by the lack of resolution of the 'quartz' component. In their place normative minerals were calculated from the bulk chemical analyses. Calcite, quartz, sericite, chlorite, kaolinite, boehmite, hematite and anatase are used to represent the mineral assemblage. Sericite (muscovite) was substituted for illite because its chemical formula is similar and more definite, and difference in normative estimates are small. Although Mg may largely be in illite, it is calculated separately as a Mg-Fe chlorite component with the composition $Mg_{8.75}Fe_{1.75}Al_{3}Si_{6.5}O_{20}(OH)_{16}$ in the chlinochlore field.

The minerals are computed in cation percent, which is close to modal estimation. Assumptions in the calculations are that Ca is converted to apatite and calcite, K and Na to sericite, Mg to chlorite (with sufficient Fe to form chlinochlore), excess Fe to hematite, Ti to anatase, excess Si and Al to kaolinite, excess Si to quartz, and excess Al to boehmite. Calcite probably contained minor Mg (shown below with mass changes), thus estimates of chlorite in the limestone and altered marl are probably high. Changes in amounts of normative minerals with increasing total wt.% Al_2O_3 in the bauxite profile are illustrated (Fig. 4).

With decreasing calcite in the above units, the argillite components, kaolinite, sericite, chlorite and quartz, are increased and reach maxima at ~28 wt.% Al_2O_3. Beyond this point lateritization in groundwater that was probably slightly acidic depleted base cations (K, Mg,

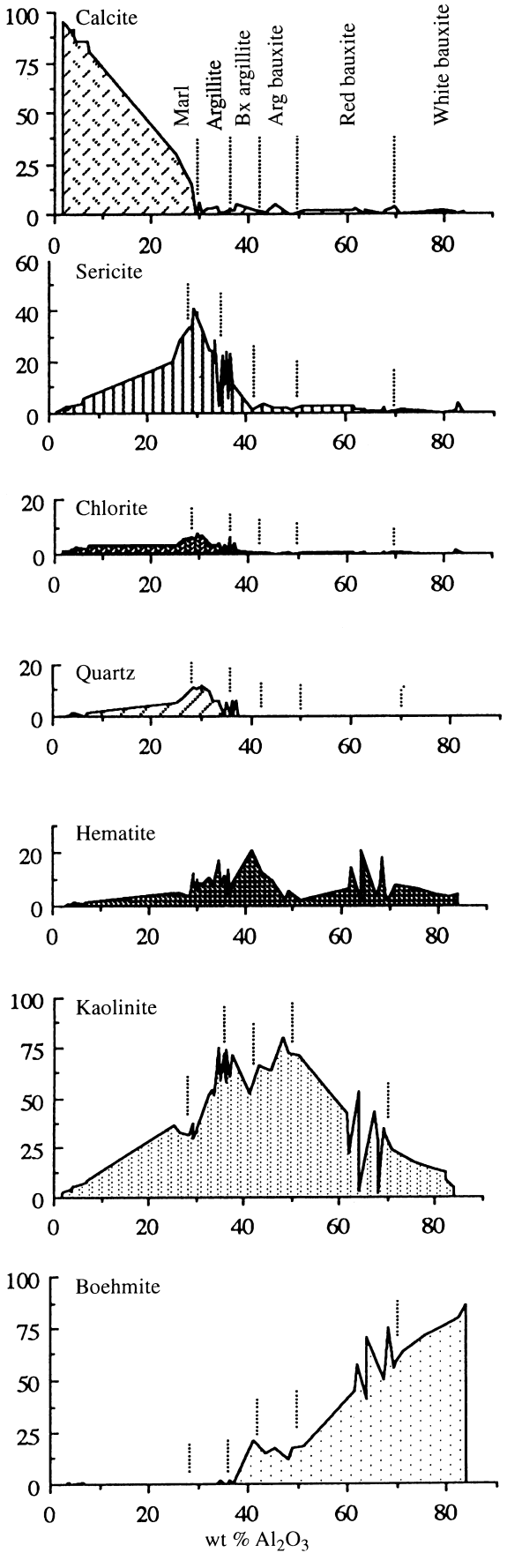

Fig. 4 Profiles of cation% normative minerals from limestone to white bauxite, plotted against total Al_2O_3 in wt.%. *Spikes* in the profiles of bauxite units are hematite-rich zones

Fe) and silica. Sericite was converted to kaolinite by the reaction:

$$\underset{\text{sericite}}{2KAl_3Si_3O_{10}(OH)_2} + 2H^+ + 3H_2O = \underset{\text{kaolinite}}{3AlSi_2O_5(OH)_4} + 2K^+ \quad (4)$$

and disappeared at ~40 wt.% Al_2O_3. Chlorite was lost in a similar reaction, and quartz was simply leached by Si-undersaturated groundwater. This produced a residue of kaolinite, hematite and minor (~2%) anatase. Where quartz was fully leached prior to completion of the breakdown of sericite and chlorite, some boehmite was produced and formed bauxitic argillite.

In the bauxite-forming stage, silica was leached from kaolinite and boehmite was formed:

$$\underset{\text{kaolinite}}{Al_2Si_2O_5(OH)_4} + 3H_2O = \underset{\text{boehmite}}{2AlO(OH)} + 2H_4SiO_4(\text{aqueous}) \quad (5)$$

Products of the early stages of this reaction resulted in the formation of argillaceous bauxite, and continued loss of silica from kaolinite produced the red and white bauxite. Hematite (and goethite) persisted through the early bauxite-forming stage, with a build-up in the red bauxite. Fe was leached at high water/rock ratios from the upper part of the profile to form white bauxite, but overall Fe was only moderately mobile during bauxitization.

The effects of the mineralogical changes are combined in Fig. 5. This diagram shows the progress of the reactions and the general tenor of the residual concentration in the kaolinization and bauxitization processes. The possibility of an excess build-up of sericite, chlorite, hematite and kaolinite over residual concentration is suggested for the marl and argillite (Figs. 4, 5).

Residual concentration: "immobile" elements

A plot of TiO_2 versus Zr (Fig. 6) produces a single trend for all units including the footwall limestone. These two elements were extremely immobile ($R = 0.992$, Table 3), and were residually concentrated in each successive unit. Ti, Zr, Nb, Cr, Th and V produce similarly well-correlated data arrays when plotted against Al (Fig. 7, Table 3). All these elements were highly immobile, but Ti has the most consistently high correlation coefficients, and it is used for mass change calculations. The small differences in scatter between pairs can be attributed to minor mobility, slight source rock inhomogeneity, or local winnowing of lateritized minerals in subaerial weathering. The latter would tend to separate heavy minerals containing Ti, Zr, Nb, etc., from the light Al-bearing kaolinite and boehmite. Only yttrium responds very differently: it is immobile in most hydrothermal alterations (R-values ~0.8 to >0.9) but was mobile (Table 3) during bauxite formation.

The plots of CaO, SiO_2, Fe_2O_3, MgO and K_2O against Al_2O_3 (Fig. 7) show large-scale mobility and

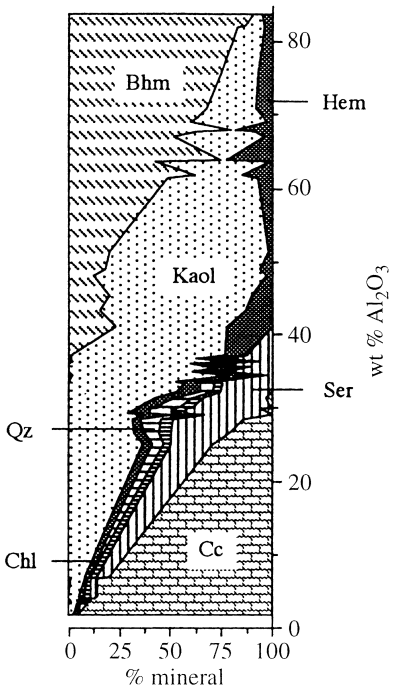

Fig. 5 Compilation profile of normative minerals plotted against total Al_2O_3 in wt.%. *Cc*, calcite; *Chl*, chlorite; *Qz*, quartz; *Ser*, sericite; *Hem*, hematite; *Kaol*, kaolinite; *Bhm*, boehmite

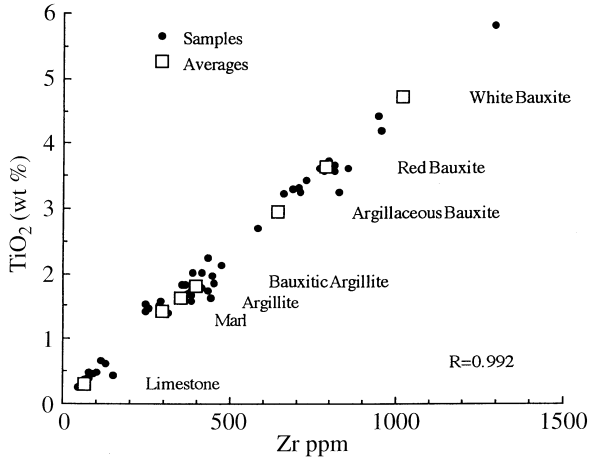

Fig. 6 Plot of TiO_2 (wt.%) versus Zr (ppm) data, with average composition shown for each sampled unit. Each element is residually concentrated at a constant TiO_2/Zr ratio. R is the correlation coefficient

ultimate depletion with increasing Al_2O_3. The drop in CaO at low Al_2O_3 values is due to the variable argillite content of the limestone, and to the degradation of altered marl during karst weathering. In our data set, marl spans the range from ~24 to 28 wt.% Al_2O_3 and marks the final stage of carbonate dissolution. SiO_2, Fe_2O_3, MgO and K_2O increase at this stage by residual enrichment to maxima in the argillite, and are then depleted. MgO and K_2O have essentially disappeared at 40 wt.% Al_2O_3, the start of boehmite formation, but Fe_2O_3 and SiO_2 diminish more gradually and are present throughout the bauxite.

Table 3 Correlation coefficients for elements in the Olmedo bauxite

	Al	V	Ti	Cr	Fe	Ni	Y	Zr	Nb	Th
Al	1.000									
V	0.939	1.000								
Ti	0.973	0.904	1.000							
Cr	0.972	0.948	0.955	1.000						
Fe	0.341	0.582	0.316	0.429	1.000					
Ni	0.257	0.241	0.210	0.263	0.510	1.000				
Y	0.000	0.000	0.000	0.000	0.539	0.344	1.000			
Zr	0.960	0.895	0.992	0.945	0.307	0.217	0.000	1.000		
Nb	0.965	0.875	0.992	0.937	0.245	0.187	0.000	0.986	1.000	
Th	0.995	0.955	0.938	0.974	0.509	0.313	0.000	0.861	0.831	1.000

Mass changes

Having shown that the argillite component of the limestone is the probable parent for the bauxite, the changes in the mobile chemical components in the lateritized samples can be calculated against Ti, the most immobile element. An example calculation is given for the conversion of argillite component of the limestone to red bauxite (Table 4). From an initial 100 g of argillite, 47.92 g of red bauxite containing 33.12 g of Al_2O_3 are produced. The largest loss of mobile material is SiO_2 (−42.79 g), followed by MgO (−5.48 g), and K_2O (−2.53 g).

Mass changes are illustrated for all units in Fig. 8. The three bauxite units at the top of the profile have lost the most mobile mass, and the argillite and altered marl units gained some mobile components. The largest change was loss of Si from the three bauxite units, and some of it was added to the argillite and altered marl below. Fe, K, Mg and a small portion of the Al were also leached in upper parts of the profile and added below. Mg appears to have been depleted throughout the profile, including the desiccated marl and argillite; much of it was probably a carbonate component in the limestone. The excessive build-ups of quartz, hematite and sericite in the argillite (Figs. 4 and 5) are confirmed here. More Al appears to have been added to argillite and altered marl than was lost from the bauxite (Fig. 8). This apparent imbalance is discussed later. The most lateritized material, the white bauxite, contains over 80 wt.% Al_2O_3 and ~4.5 wt.% TiO_2 (Table 2b).

Discussion

Source material

Owing to the nature of karst erosion, where both chemical and mechanical weathering are active, it is ordinarily difficult to determine if one or more sources of argillaceous debris were converted to bauxite. Potential sources of debris are the underlying shallow marine argillaceous limestone, fluviatile sediment washed in from a hinterland at the time of karst weathering, and volcanic ash. Immobile elements in each of these three possible sources would have different distributions. If each source was homogeneous, three separate linear trends would be generated for each element pair. If one or more of the sources were heterogeneous, a fan or random distribution of data would be generated (MacLean 1990). As only one highly correlated trend is present for each immobile element pair (Figs. 6 and 7), it is evident that only one homogeneous source existed, and it coincides with the linear trends of the argillaceous limestone. The argillite in the limestone is a detrital component that was probably derived from a wide and variable source, and homogeneously mixed prior to deposition.

Bauxite genesis

Bauxitization of argillite debris derived from the footwall limestone proceeded from the surface downward with the build-up of an upper layer of residual "immobile" components (Al, Ti, Zr, Th, Nb, etc., Table 4). Between 25 and 50 m of argillaceous limestone was required to form the equivalent of one meter of pure Al_2O_3 in the bauxite zone of the profile (Fig. 9). Portions of the K, Si, Fe, Mg and Al that were leached near the ground surface moved downward into the argillite and altered marl and were precipitated largely as quartz and illite. Thus, while the top of the argillite was being converted to bauxite minerals, small amounts of argillite minerals were being added below. These reprecipitated components add extra texture and color to the argillite and altered marl. During the process, iron was only moderately soluble and was irregularly concentrated as hematite and minor goethite in red bauxite and argillaceous bauxite. The mottled distribution of Fe-rich and Fe-poor domains (red and white; Fig. 3) is typical of a leached profile that was undisturbed by mechanical weathering.

Argillaceous bauxite forms both abrupt and gradational boundaries with red and white bauxite. Its lower boundary is defined by the closely spaced disappearances of illite (sericite, chlorite) and quartz which coincide approximately with the appearance of boehmite (Figs. 4, 5). The boehmite-forming reaction (Eq. 5) proceeds only in a quartz-free system, hence the appearance of boehmite, under equilibrium conditions, may take place either slightly before or after the sericite and chlorite (illite) are fully consumed.

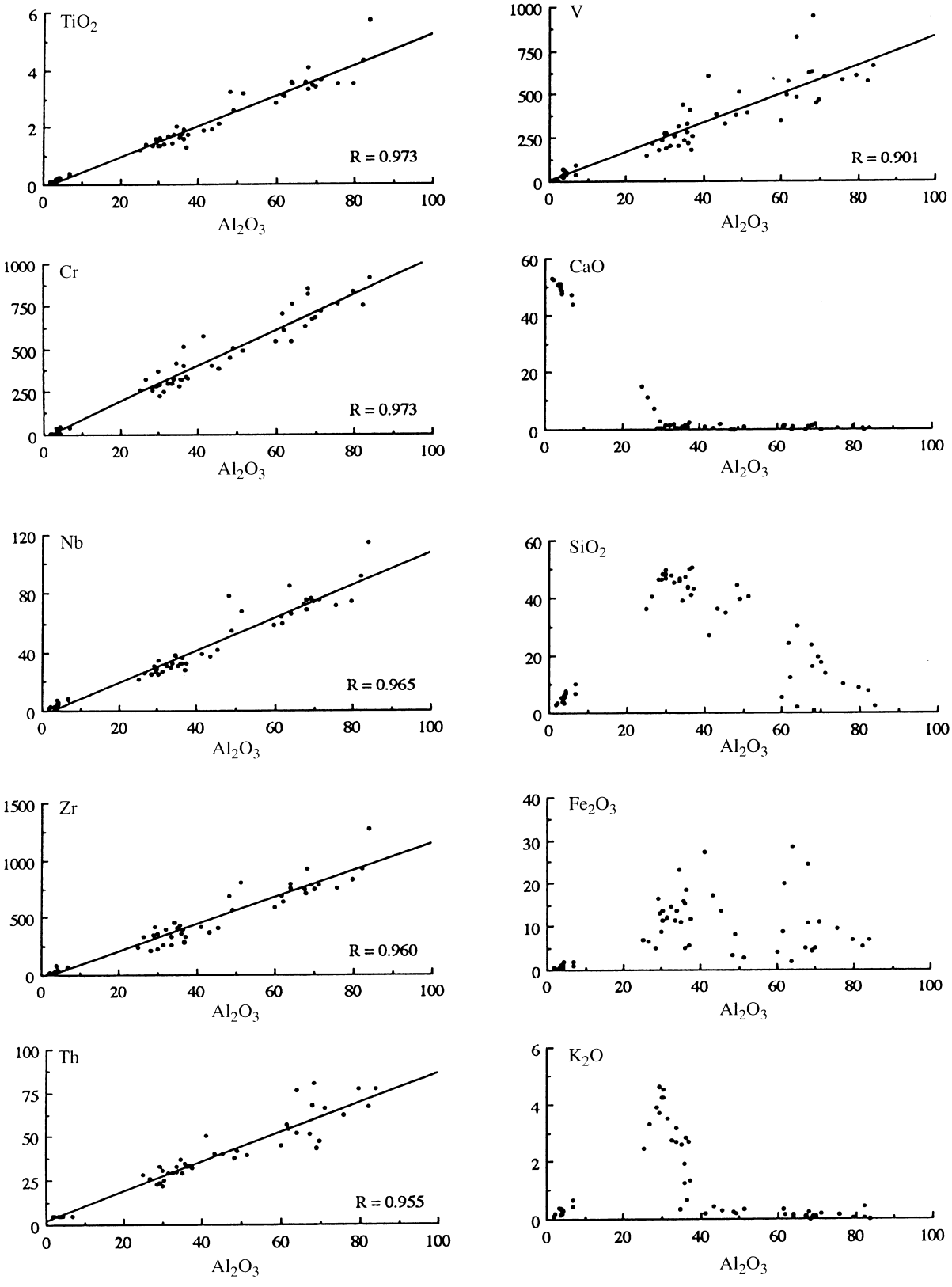

Fig. 7 Binary plots of some major elements (wt.%) and trace elements (ppm) against Al_2O_3 (wt.%). Well-correlated sample data denote immobile element pairs. CaO, SiO_2, Fe_2O_3 and K_2O were mobile and eventually depleted in the bauxite

Table 4 Mass change owing to conversion of average argillite in argillaceous limestone to red bauxite (data from Table 2b). The changes, based on TiO_2 as the immobile component, are listed in weight percent (or grams). *RC* is the *reconstituted composition* of the red bauxite, and *EF* is the *enrichment factor*

	Argillaceous limestone	Red bauxite	*RC*	Mass change
SiO_2	46.58	7.91	3.79	−42.79
TiO_2	1.73	3.61	1.73	0.00
Al_2O_3	33.99	69.11	33.12	−0.87
Fe_2O_3	9.05	19.10	9.15	+0.10
MnO	0.26	0.02	0.01	−0.25
MgO	5.52	0.08	0.04	−5.48
CaO	0.00	0.00	0.00	0.00
Na_2O	0.14	0.00	0.00	−0.14
K_2O	2.58	0.11	0.05	−2.53
P_2O_5	0.15	0.06	0.03	−0.12
Total	100.00	100.00	47.92	−52.08
EF			0.4792	

Mobility of aluminium

The downward movement of small amounts of Al within the bauxite profile is well established by this study. Al was removed mainly from the white bauxite and added to the argillite and altered marl (Fig. 8). Al is least soluble in neutral pH groundwater, hence its downward migration in solution may have been enhanced by seasonal fluctuations in the acidity of saline groundwater (Brimhall et al. 1988).

Downward filtration of fine bauxite-rich sediment might also be a mechanism of Al and Fe migration, but this process should also transport immobile element-rich heavy minerals (anatase, zircon, etc.) as well. Preferential erosion of the low density bauxite minerals by wind action, and their subsequent redeposition, a mechanism proposed by Brimhall et al. (1988) and Pye (1988) for the formation of some Al-rich bauxite deposits, could account for losses and gains of Al in the white bauxite horizon. Although this process could extract Al from the white bauxite (Fig. 8), it is not one that could easily add Al to the underlying argillite and altered marl. Wind erosion should favor loss of the light bauxite minerals over heavier ones, and produce anomalous scatter on Zr- Al_2O_3 or other plots. It follows that deposits formed from windborne bauxite should be depleted in the heavy minerals.

Mass changes

The procedures used to calculate mass changes and minor mobility of Al were possible only because the precursor argillite was very homogeneous and the immobility of a number of elements could be rigorously proven. That Al moved downward in the bauxite profile seems probable, but it is in apparent imbalance between Al depleted from the white bauxite and that added to the argillite and marl (Fig. 8). These profiles of mass change

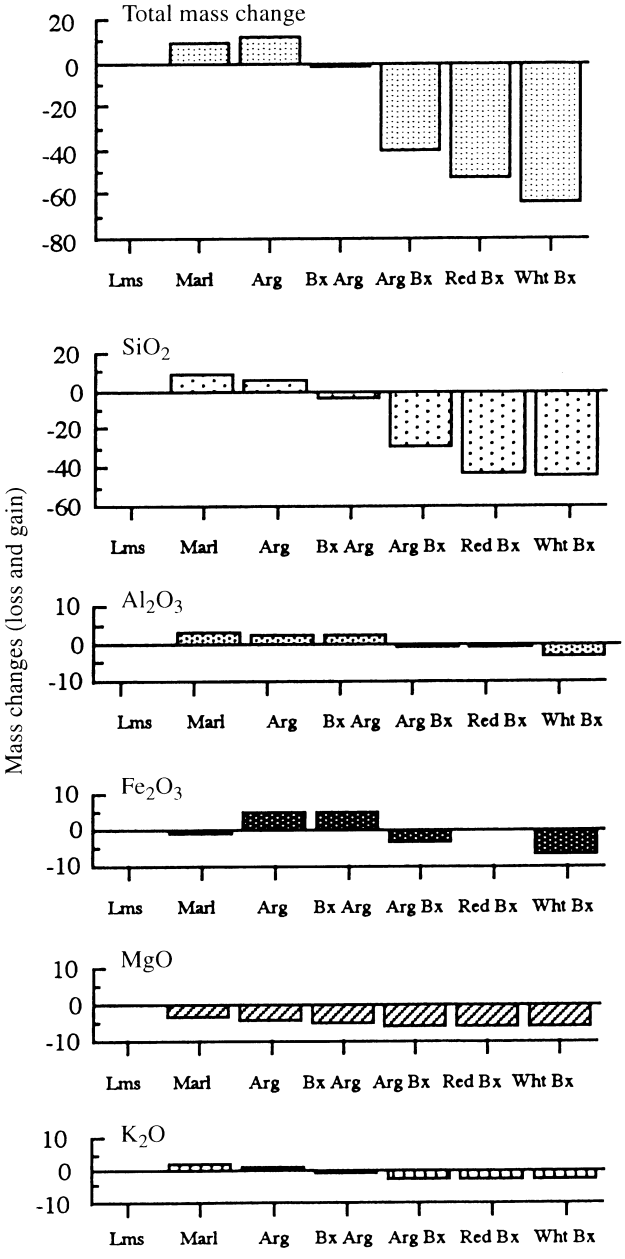

Fig. 8 Mass changes relative to the argillite component of the footwall limestone. The changes can be considered as gains and losses in wt.%, or grams per 100 grams of argillite precursor

(Fig. 8) are derived from average chemical compositions, and do not factor ('weight') sizes (mass or volume) of units. However, this can be evaluated. Layered units in stratiform deposits have the same or similar lateral extents, hence mass differences are largely functions of thickness. By 'weighting' the chemical analyses to the thicknesses of units in the bauxite profile (Fig. 10), the mass changes more-or-less balances between loss of Al in the bauxite and gain of Al in argillite and altered marl. From these data it is estimated that 1.2 wt.% of Al_2O_3 available for concentration in the bauxite was mobilized and moved downward into the argillite and marl.

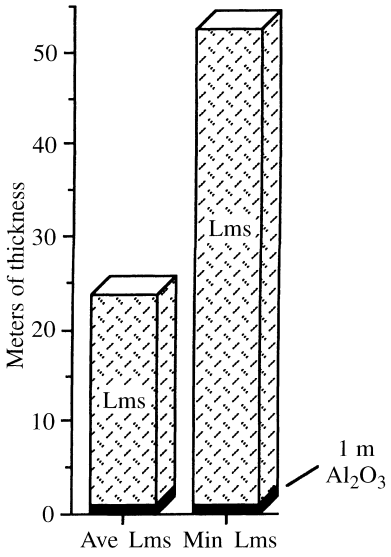

Fig. 9 Estimate of the height of the footwall limestone column to produce 1 m of Al_2O_3, based on (a) average argillite content of the limestone, and (b) minimum argillite content

Conclusions

Karst weathering had produced a layer of argillaceous debris on top of early Cretaceous limestone, and lateritization partially converted this debris to bauxite. Al and small amounts of Ti, Zr, Nb, Th, Cr, V and Fe were residually accumulated at the top of the weathering profile during the lateritization. Boehmite, kaolinite, hematite and minor anatase constitute the bulk of the bauxite horizon. Plots of the accumulated elements, except Fe, produce highly correlated linear trends, proof they were immobile during the bauxite-forming process and derived from a homogeneous source. Immobile element ratios and distributions show that the altered marl, argillite and bauxite were derived from the underlying argillaceous limestone and marl. The immobile elements are also used to quantify the losses of mobile material (SiO_2, MgO, K_2O, etc.). Although most mobile rock material was removed from the system, considerable Si, Mg, K, Fe and minor Al seeped downward and were precipitated as illite (sericite, chlorite), hematite and quartz or amorphous silica. An estimated 1.2 wt.% of Al_2O_3 originally available in the bauxite was moved into the argillite and altered marl units.

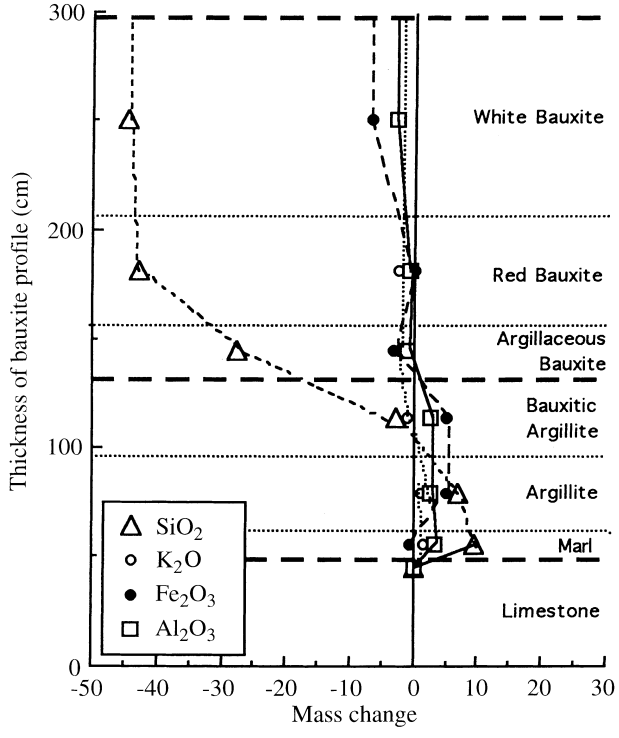

Fig. 10 Mass changes versus thickness of the bauxite profile (from Fig. 3). Note that the depletion of Al_2O_3 in the bauxite units is approximately offset by Al_2O_3 gains in the argillite-marl zones

Acknowledgements We thank PROGEMISA for permission to carry out this study on the Olmedo Deposit. A review of an early version of the manuscript by N. Bliss and L. Wickert, Alcan Limited, and comments by the journal referees are appreciated. Chemical analyses at McGill University were financed by National Recearch Council of Canada Grant A7719.

References

Bárdossy G (1982) Karst Bauxites. Elsevier Scientific, Amsterdam, 441 p

Bárdossy G (1984) European bauxite deposits. In: Leonard Jacob Jr (ed), Bauxite, Proc 1984 Bauxite Symposium, Los Angeles, California. Society of Mining Engineers, New York, pp 411–435

Brimhall GH, Lewis CJ, Ague JJ, Dietrich, WE, Hampel J, Rix P (1988) Metal enrichment in bauxites by deposition of chemically mature aeolian dust. Nature 333: 819–824

Cocco G, Pecorini G (1959) Osseovazioni sulfe bauxite delle Nurra (Sardenge Sud-Ocendentale). Mem Soc Geol Italia 6(4): 607–642

Gow NN, Lozej GP (1993) Bauxite. Geosci Can 20: 9–16

Lyew-Ayee PA (1986) A case for the volcanic origin of Jamaican bauxites. Proc Bauxite Symposium VI, 1986. J Geol Soc Jamaica 9–39

MacLean WH, Kranidiotis P (1987) Immobile elements as monitors of mass transfer in hydrothermal alteration: Phelps Dodge massive sulfide deposit, Matagami, Quebec. Econ Geol 82: 951–962

MacLean WH (1990) Mass change calculations in altered rock series. Mineral Deposita 25: 44–49

MacLean WH, Barrett TJ (1993) Lithogeochemical techniques using immobile elements. J Explor Geochem 48: 109–133

Oggiano G, Sanno G, Temussi I (1987) Caractere geologiques et geochemiques de la bauxite de la Nurra. In: Cherchi A (ed) Excursion en Sardenge, Mai, 1987, Departement de Science de la Terre de Cagliari

Pye K (1988) Bauxites gathering dust. Nature 333: 300–301

Sanna G, Temussi I (1986) La minera di bauxite di Olmedo. Ind Miner 6: 7–42

Sastri, GGK, Sastry CS (1982) Chemical characteristics and evolution of the laterite profile in Hazaridadar Bauxite Plateau, Madhya Pradesh, India. Econ Geol 77: 154–161

Valeton I, Biermann M, Reche R, Rosenberg F (1987) Genesis of nickel laterites and bauxites in Greece during the Jurassic and Cretaceous, and their relation to ultrabasic parent rocks. Ore Geol Rev 2: 359–404